

Realization and Simulation a Novel Kind of Parallel Cables-Based Robot with Five Cables

FOUED INEL¹, MOHAMMED KHADEM², ABDELGHAFOUR SLIMANE TICH TICH³

¹Mechanical Engineering Department, Automatic Laboratory, University of Skikda, ALGERIA

²Mechanical Engineering Department LGMM Laboratory, University of Skikda, ALGERIA

³Mechanical Engineering Department LGMM Laboratory, University of Skikda, ALGERIA

Abstract. In this paper, we introduce the pyramidal robot, a novel kind of parallel cable-based robot that has been constructed and designed with five cables. Last, we suggested a control method. In this context, we studied the application of the Runge-Kutta method of fourth order for resolving the non-linear partial differential equations of our system, which is frequently employed for managing uncertainties in linear systems. The primary contribution of this study is firstly the design of a reel prototype and the creation and implementation of a graphical user interface (GUI) for displaying the position of the end effector. Second, to test the precision of the tracking of the object, we analyse the system's response using cutting-edge methods such as predictive control. Finally, using the advanced technique proposed, we present the simulation results on this cable-based robot. These results demonstrate the performance of the technique as proposed.

Key Words: Dynamical Systems, Robotics, Cable based parallel robot; simulation; Predictive control; GUI.

Received: April 8, 2022. Revised: October 25, 2022. Accepted: November 21, 2022. Published: December 31, 2022.

1 Introduction

cable-based parallel robots are a unique type of parallel manipulators robot in which the end-effectors are powered by cables instead of rigid links [1-3] and The movement is given by the winding and unwinding of cables [2, 8, 9]. When compared to the robots of traditional architecture, these provide undeniable advantages [4-7]. This last device is a sort of parallel manipulator that connects a fixed base to a movable platform using cables [10, 11]. The coordinate controller of cable lengths and tensions permit the displacement and the application of efforts on the platform. These robots have few moving parts, with reduced mass, and are most suitable for tasks requiring high performance such as speed and accuracy and provide a large workspace. By moving the cable's connection points, it is possible to obtain reconfigurable manipulators. In addition, they are easy to mount; dismount and transport, in other hand, the main disadvantages of parallel manipulators lie in the nature of the cables that can only work in one direction rather than the traction [12-14]. The best-known application is the Skycam, a camera controlled by a cable mechanism that is used for tele-diffusion of professional football games. Another area of interest in biomedical applications such as tracking the movement of body parts. An example is the CaTraSys (Cassino Tracking System) was used for the identification of

kinematic parameters and the mobility of man [15, 16].

The unique parallel manipulators known as cable-based parallel robots a suitable control technique is essential for cable-based robots in order to achieve proper motions without damaging the cables.

According to reports like those in [17-19,20], the Predictive approach has been created to increase the robustness of robotic system control. An adaptive predictive controller in particular can adjust the control torque based on current position. The purpose of this work is fulfilled through the design of a new prototype pyramidal cable-based robot with five cables, followed by the implementation of dynamics modelling with a predictive controller for control on real. Finally, simulation results have been applied to verify and assess the suggested the algorithm performs.

2 System Description

Figure 1 shows our reel prototype robot with five cables. The base is fixed and each cable is attached to the one end of the platform. As a result of motor moments, cable wraps and winds the cables around the pulley to control the position and the orientation of the end-effector. The five cables-based robots allow a 3D plane movement with 5 degrees of freedom and figure 2 shows the general geometrical axes and the vector analysis

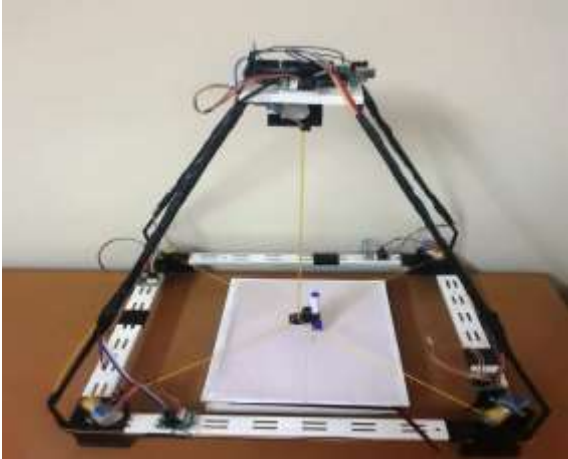


Fig 1: A Reel prototype pyramidal based parallel robot

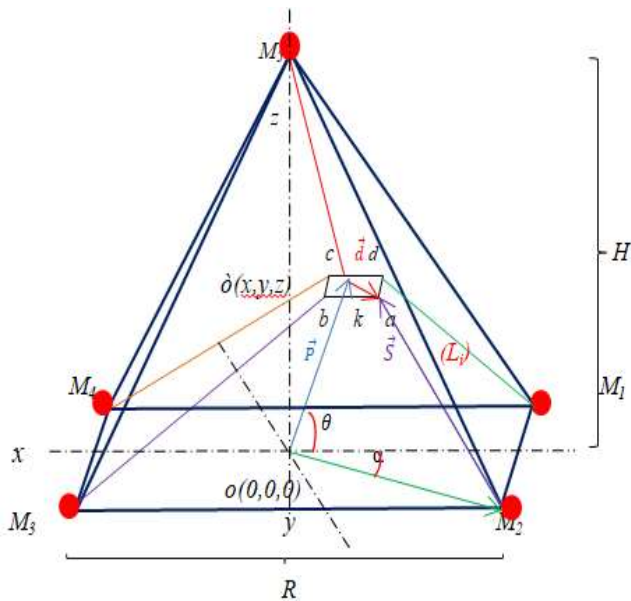


Fig 2: The general geometrical axes and the vector analysis

With:

The geometric parameters that describes the robot are listed in the following :

L_i : length of the cable;

\mathcal{R}^* : Unitary matrix ;

R : side length of the robot base (The shape of the robot base is square) ;

H : height between the base and the motor S_5 ;

M_i : exit point of the cables from the base;

\vec{s}_i : vector to $(a, M1)$;

\vec{p}_i : vector to (\dot{o}, o) ;

\vec{a}_i : vector to $(M1, o)$;

\vec{d}_i : vector to (a, \dot{o}) .

k : is the side length of the end-effector (The shape of the end-effector is square).

3 Geometric Modelling

In this section, we present the inverse geometric model for five cable-based robots.

3.1 Establishment of Mathematical Model

This model aims to determine the lengths of the cables " L_i ", the angles " Θ_i " between the X,Y axes and the cables connected to the mobile platform and " α_i " between the Z axis and the plane axes (X, Y). The inverse geometric model can be expressed by the following equations [21].

$$L_i = \sqrt{(x - A_{ix})^2 + (y - A_{iy})^2 + (z - A_{iz})^2} ;$$

$$i=1...5. \quad (1)$$

$$\Theta_i = \arctan g\left(\frac{y - A_{iy}}{x - A_{ix}}\right)$$

$$; i=1...5. \quad (2)$$

$$\alpha_i = \arctan g\left(\frac{z - A_{iz}}{\sqrt{(x - A_{ix})^2 + (y - A_{iy})^2}}\right)$$

$$; i=1...5. \quad (3)$$

4 The Dynamic Modelling

In this section, we begin to present the dynamic equation for a robot with five cables and its state-space representation. Then, the response will be simulated in a closed loop with a predictive controller as a method [22].

4.1 Establishment of Mathematical Model

The dynamic model of the actuator can be expressed by the following equation according to the structure pulley as illustrated in figure 2 [23]:

$$m \ddot{X} = F_R \quad (4)$$

Where: m is the mass matrix and \ddot{X} is the acceleration vector of the end-effector.

$F_R = (F_{R_x} \quad F_{R_y} \quad F_{R_z})^T$: is the resultant force of all tensions applied to the cables.

$$\text{Where: } \begin{pmatrix} m & 0 & 0 \\ 0 & m & 0 \\ 0 & 0 & m \end{pmatrix} \begin{pmatrix} \ddot{x} \\ \ddot{y} \\ \ddot{z} \end{pmatrix} = \begin{pmatrix} F_{R_x} \\ F_{R_y} \\ F_{R_z} \end{pmatrix}$$

(5)

4.2 The Dynamic Comportment of the Motors

Figure 3 shows the structure pulley and its dynamic comportment is expressed by the following equation:

$$J \ddot{\beta} + C \dot{\beta} = \tau - rT. \quad (6)$$

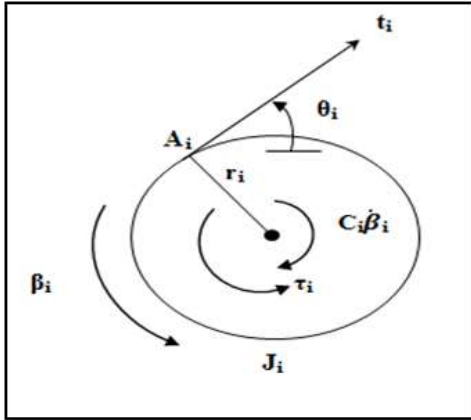


Fig. 3: Structure pulley.

with:

$$Jmat = \begin{pmatrix} J_1 & 0 & 0 & 0 \\ 0 & J_2 & 0 & 0 \\ 0 & 0 & J_3 & 0 \\ 0 & 0 & 0 & J_4 \end{pmatrix} \text{ and } Cmat = \begin{pmatrix} C_1 & 0 & 0 & 0 \\ 0 & C_2 & 0 & 0 \\ 0 & 0 & C_3 & 0 \\ 0 & 0 & 0 & C_4 \end{pmatrix} \quad (7)$$

We consider that all the rays of the pulley are the same:

$$r_i = r \quad (i=1,2,\dots,5),$$

$\tau = (\tau_1, \tau_2, \dots, \tau_i)^T$: is the vector of the torques applied by the motors.

$t = (t_1, t_2, \dots, t_i)^T$: is the vector of tension cables.

β : is the angle of rotation of the pulley.

θ_i : The angles between cables and the pulley.

So:

$$t = \frac{1}{r} (\tau - J \ddot{\beta} - C \dot{\beta}). \quad (8)$$

Where L_{i0} are the initial lengths of the cables:

$$L_{i0} = \sqrt{(Aix)^2 + (Aiy)^2 + (Aiz)^2}$$

So

$$\beta = \begin{pmatrix} \beta_1(X) \\ \beta_2(X) \\ \vdots \\ \beta_i(X) \end{pmatrix} = \frac{1}{r} \begin{pmatrix} L_{10} - L_1 \\ L_{20} - L_2 \\ \vdots \\ L_{i0} - L_i \end{pmatrix}. \quad (9)$$

$i=1, \dots, 5$

$$\dot{\beta} = \frac{\partial \beta}{\partial x} \dot{x} = -\frac{1}{r} \begin{pmatrix} \cos(\alpha_1) \cos(\theta_1) & \cos(\alpha_1) \sin(\theta_1) & \sin(\alpha_1) \\ \cos(\alpha_2) \cos(\theta_2) & \cos(\alpha_2) \sin(\theta_2) & \sin(\alpha_2) \\ \cos(\alpha_3) \cos(\theta_3) & \cos(\alpha_3) \sin(\theta_3) & \sin(\alpha_3) \\ \sin(\alpha_4) \cos(\theta_4) & \sin(\alpha_4) \sin(\theta_4) & \cos(\alpha_4) \end{pmatrix} \begin{pmatrix} \dot{x} \\ \dot{y} \\ \dot{z} \end{pmatrix} \quad (10)$$

by subtracting successively (10) with respect to time, we get:

$$\ddot{\beta} = \frac{d}{dt} \left(\frac{\partial \beta}{\partial x} \right) \dot{x} + \frac{\partial \beta}{\partial x} \ddot{x} \quad (11)$$

Substituting (11) we obtain:

$$t = \frac{1}{r} \left(\tau - J \left(\frac{d}{dt} \left(\frac{\partial \beta}{\partial X} \right) \dot{X} + \frac{\partial \beta}{\partial X} \ddot{X} \right) - C \frac{\partial \beta}{\partial X} \dot{X} \right) \quad (12)$$

Finally, the set the equation of the dynamic model can be expressed in a standard form for robotic systems (13):

$$\ddot{X}(t) = M^{-1}(X) * N(X, \dot{X}) + M^{-1}(X) * S(X) * \tau \quad (13)$$

Where:

$$M = r * m + S(X) J \frac{\partial \beta}{\partial X} \quad (14)$$

And

$$N(X, \dot{X}) = S(X) \left(J \frac{d}{dt} \frac{\partial \beta}{\partial X} + C \frac{\partial \beta}{\partial X} \dot{X} \right) \quad (15)$$

$$\tau = \begin{pmatrix} \tau_1 \\ \tau_2 \\ \vdots \\ \tau_i \end{pmatrix} \quad i=1, \dots, 5 \quad (16)$$

6 Control ONTROL Law and Architecture

This section, the low-level control, has been ensured by the development of a model Predictive control based on the overall system Cartesian Dynamics Equations of Motion, which is presented in this section (Equation 13). In his paper on the MPC gains are determined the error using a Matlab program simulation to achieve reasonable performance for the trajectories. The establishment of the control law along X,Y and along Z is: Consider the following MIMO nonlinear system:

Consider the following MIMO nonlinear system.

$$\begin{cases} \dot{x} = F(x) + \sum_{i=1}^m g_i(x)u_i = F(x) + G(x)U \\ y = h(x) = [h_1(x), h_2(x), \dots, h_m(x)]^T \end{cases} \quad (17)$$

Where $x \in R^n$, $U \in R^m$ and $y \in R^m$ are, respectively, the state vector, the control vector and the output vector. $F(x)$ and $h(x)$ are smooth vector fields.

Predictive controller is designed such that the future output $y(t+T)$ follows the future reference signal $y_r(t+T)$ minimizing the quadratic performance index given below:

$$J = \int_0^T e(t + \tau)^T e(t + \tau) d\tau \quad (18)$$

Where:

$e(t+T)$ is the future tracking error vector, and $T > 0$ is the prediction horizon.

The outputs of the system and the reference signals predictions are approximated by their Taylor-series expansions up to corresponding relative degree ρ_i :

$$e_i(t + T) \approx \sum_{k=0}^{\rho_i} \frac{T^k}{k!} (y_{r_i}^{(k)}(t) - y_i^{(k)}(t)) \quad (19)$$

$$e_i(t + T) \approx \begin{bmatrix} 1 & T & \frac{T^2}{2!} & \dots & \frac{T^{\rho_i}}{\rho_i!} \end{bmatrix} \begin{bmatrix} y_{r_i}(t) - y_i(t) \\ \dot{y}_{r_i}(t) - \dot{y}_i(t) \\ \ddot{y}_{r_i}(t) - \ddot{y}_i(t) \\ \vdots \\ y_{r_i}^{(\rho_i)}(t) - y_i^{(\rho_i)}(t) \end{bmatrix} \quad (20)$$

$$e_i(t + T) = \Gamma_i(T)Y_i(t)$$

The outputs y_i time derivatives required in the approximated performance index are ex-pressed as given below using Lie derivatives [25]:

$$\begin{cases} \dot{y}_1 = L_F h_1(x) \\ \ddot{y}_1 = L_F^2 h_1(x) \\ \vdots \\ y_1^{(\rho_1)} = L_F^{\rho_1} h_1(x) + L_{g_1} L_F^{\rho_1-1} h_1(x)u_1 + \dots + L_{g_m} L_F^{\rho_1-1} h_1(x)u_m \\ \dot{y}_2 = L_F h_2(x) \\ \vdots \\ y_2^{(\rho_m)} = L_F^{\rho_m} h_m(x) + L_{g_1} L_F^{\rho_m-1} h_m(x)u_1 + \dots + L_{g_m} L_F^{\rho_m-1} h_m(x)u_m \end{cases} \quad (21)$$

Introducing (21) in the approximated performance index (22) yields:

$$J \approx (A(x) - B(x, U))^T \Pi(T)(A(x) - B(x, U)) \quad (22)$$

Finally, the control law minimizing the approximated performance index is obtained by solving the system:

$$\frac{dJ}{dU} = \left(\frac{d(A(x) - B(x, U))}{dU} \right)^T \Pi(T)(A(x) - B(x, U)) = \mathbf{0}_{(\rho+m) \times 1} \quad (23)$$

Consequently, the control law is given by [25]:

The control architecture as shown in Figure 4 is made up of three different parts: the Predictive controller, the tension calculation and pulley angle β to determine the cable lengths L_i .

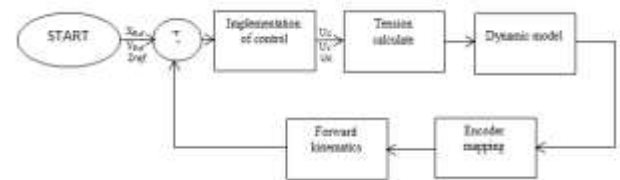


Fig. 4: Control Architecture.

7 Simulation Results

In this part, we present the simulation of the response for a 3D cables-based robot with 4 cables, for dynamic equation, which has a non-linear equation system, for this purpose, we use a Runge Kutta method as a numeric solution. Runge and Kutta developed the following formulae [26]:

$$y(x_1) \approx y_0 + (k_1 + 2k_2 + 2k_3 + k_4)/6,$$

$$k_1 = hf_0, \quad f_0 \approx f(x_0, y_0),$$

$$k_2 = hf(x_0 + h/2, y_0 + k_1/2),$$

$$k_3 = hf(x_0 + h/2, y_0 + k_2/2),$$

$$k_4 = hf(x_0 + h, y_0 + k_3).$$

And we then implement a Cartesian Predictive controller in this dynamic equation for reduce the

tracking error ($e_r = \text{desired} - \text{actual}$) for all the axes. The parameters for the dynamics equations of motion (15) for the 5cables are: point mass $m = 0.01$ kg; rotational shaft/pulley inertias J_i ($i = 1, \dots, 5$) = 0.0008 kgm²; shaft rotational viscous damping coefficients C_i ($i = 1, \dots, 5$) = 0.01 Nms and $r_i = r = 1$ cm (for all $i = 1, \dots, 5$).

Therefore, we placed the system's reference in the workspace's middle (0,0,0). Figures 5, 6 and 7 illustrate a graphical user interface for the point-to-point command, allowing the user to input any point's coordinates into the workspace, this last, the end effector is moved precisely to this point when the plot is clicked, and this interface can initialize the robot's case (Figure 8). These techniques are based on the inverse geometric model. Finally, Figures 9 and 10 show the end effector's path for different tests and plot the point when the values for the z-axes are given.

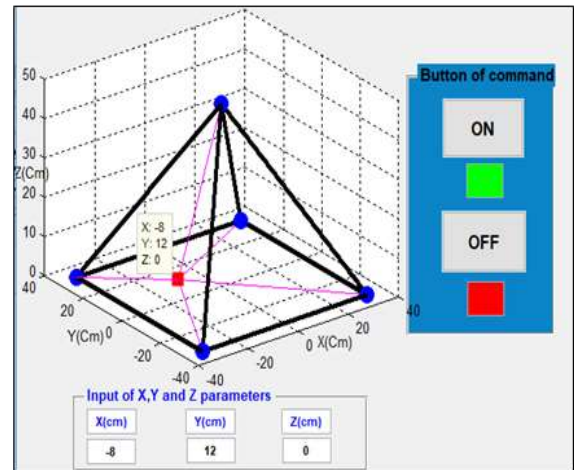


Fig. 7: Plot the end effector's displacement to position three

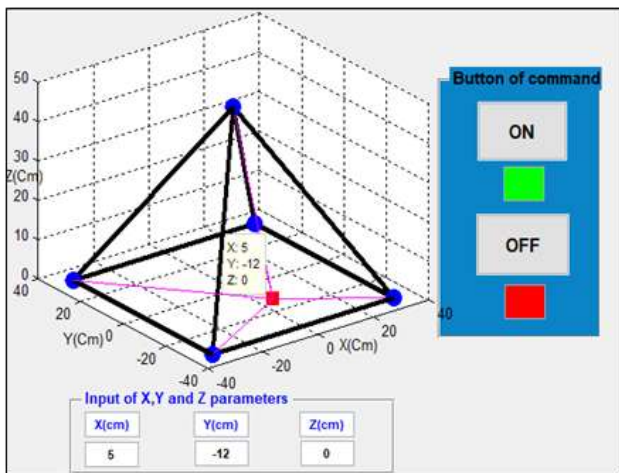


Fig. 5: Plot the end effector's displacement to position one

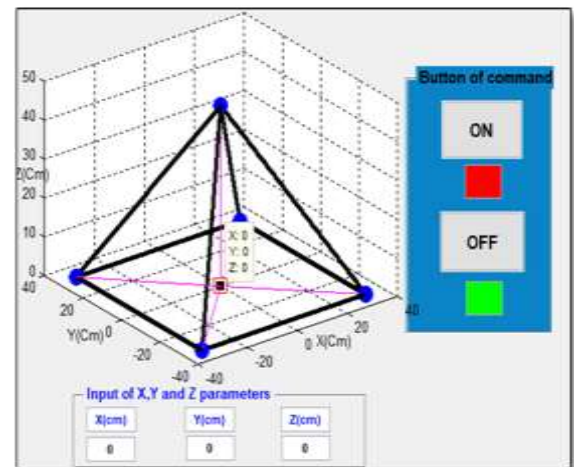


Fig. 8: Plot initialization the end effector

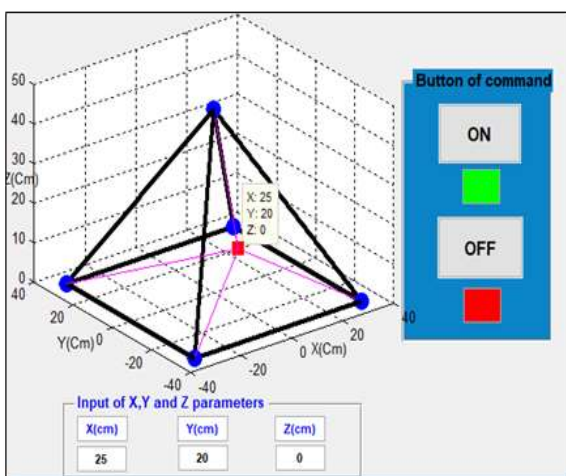


Fig. 6: Plot the end effector's displacement to position two.

When clicked on the plot, the end effector is displaced directly to this target point with a high precision, and also, this interface can initialize the case of this robot (Figure 8), this technique based on an inverse geometric model. Finally, Figures 9 and 10 show the end effector's path for different tests and plot the point when the values for the z-axes are given.

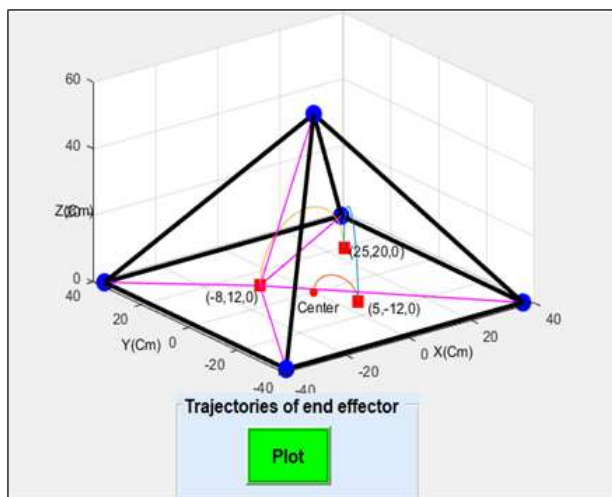


Fig. 9: Plot the end effector's path for different tests

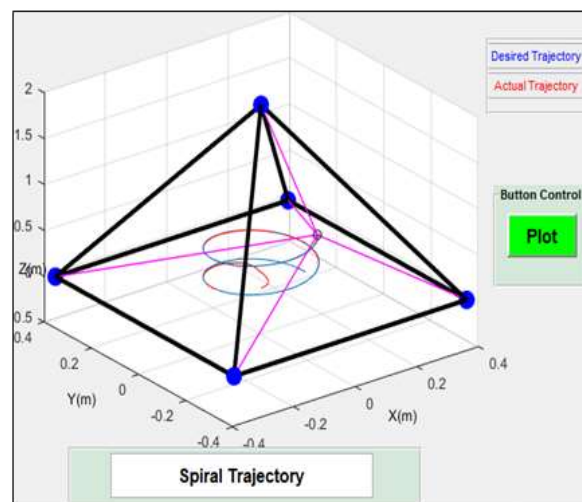


Fig.11: Plot the spiral trajectory

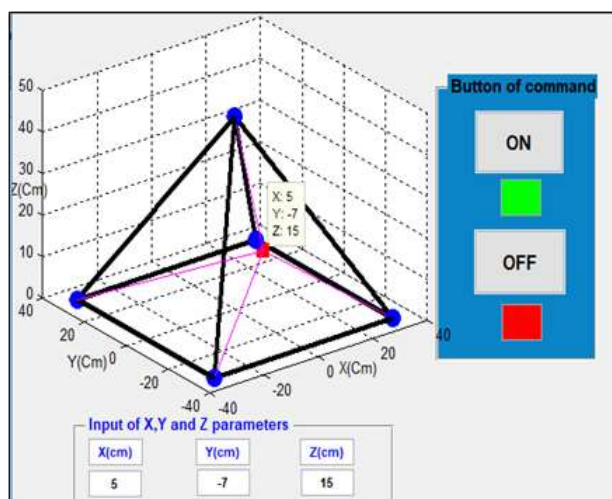


Fig. 10: Plot the point when the values for the z-axis is given

To illustrate the effectiveness of our control, we use another interface graphic command that follows a continuous trajectory. When we click on the plot, the end effector moves and precisely follows the predetermined trajectory in the workspace, as seen in figure 11. Figure 12 shows the cable lengths necessary to draw a spiral trajectory. According to the results of various tests, this predictive control performs better under most operating conditions.

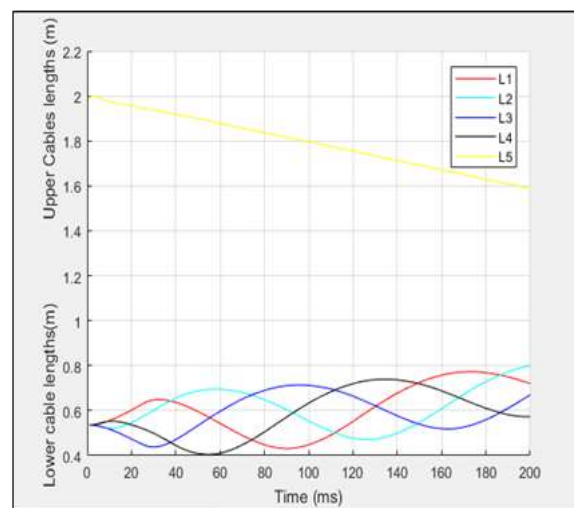


Fig. 12: Plot the cables lengths necessary to draw a spiral trajectory

8 Conclusions

This paper presented a reel prototype of a novel 3D cable base robot with five cables, this last, we have applied simulation results for different tests. In this way, we have designed predictive technique as a control, then we developed an user interface graphic with a simulation program to control the displacement of end effector based on: point to point command and according to the a predefined trajectory, we assume that, the tensions values are limited with t_{min} and t_{max} witch are always positive and the cables lengths do not exceed the workspace. Also, we have presented some results for continuance trajectories. The simulation results have demonstrated the effectiveness and feasibility of the proposed control and are suitable for improving the performance response.

References:

- [1] Zhang, J., X. Fang, and L. Qi, Sensitivity-analysis based method in single-robot cells cost-effective design and optimization. *Robotics and Computer-Integrated Manufacturing*, 2016. 38: p. 9-15.
- [2] Inel, F., et al., Dynamic Modeling and Simulation of Sliding Mode Control for a Cable Driven Parallel Robot, in *New Advances in Mechanism and Machine Science*. 2018, Springer. p. 413-426.
- [3] Fernini, B., M. Temmar, and M.M. Noor, toward a dynamic analysis of bipedal robots inspired by human leg muscles. *Journal of Mechanical Engineering and Sciences*, 2018. 12(2): p. 3593-3604.
- [4] Bonilla, D., Fuel demand on UK roads and dieselisation of fuel economy. *Energy Policy*, 2009. 37(10): p. 3769-3778.
- [5] Abd Elhakim L, "Nonexistence Results of Global Solutions for Fractional Order Integral Equations on the Heisenberg Group", *WSEAS Transactions on Systems*, vol. 21, pp. 382-386,2022.
- [6] Nongluk Viriyapong, "Modification of Sumudu Decomposition Method for Nonlinear Fractional Volterra Integro-Differential Equations", *WSEAS Transactions on Mathematics*, vol. 21, pp. 187-195, 2022.
- [7] Zi, B. and S. Qian, Introduction, in *Design, Analysis and Control of Cable-suspended Parallel Robots and Its Applications*. 2017, Springer Singapore: Singapore. p. 1-20.
- [8] Mottola, G., C. Gosselin, and M. Carricato, Dynamically feasible motions of a class of purely-translational cable-suspended parallel robots. *Mechanism and Machine Theory*, 2019. 132: p. 193-206.
- [9] Bruckmann, T., et al. Concept Studies of Automated Construction Using Cable-Driven Parallel Robots. in *Cable-Driven Parallel Robots*. 2018. Cham: Springer International Publishing.
- [10] Bruckmann, T., et al. Concept Studies of Automated Construction Using Cable-Driven Parallel Robots. in *Cable-Driven Parallel Robots*. 2018. Cham: Springer International Publishing.
- [11] Ko, S.Y., et al., Cable-driven parallel robot capable of changing workspace. 2018, Google Patents.
- [12] Williams II, R.L., J.S. Albus, and R.V. Bostelman, 3D Cable-Based Cartesian Metrology System. *Journal of Robotic Systems*, 2004. 21(5): p. 237-257.
- [13] Wang, K., et al., Endovascular intervention robot with multi-manipulators for surgical procedures: Dexterity, adaptability, and practicability. *Robotics and Computer-Integrated Manufacturing*, 2019. 56: p. 75-84.
- [14] Washabaugh, E.P., et al., A portable passive rehabilitation robot for upper-extremity functional resistance training. *IEEE Transactions on Biomedical Engineering*, 2019. 66(2): p. 496-508.
- [15] Ottaviano, E., et al., Catrasy (cassino tracking system): A wire system for experimental evaluation of robot workspace. *Journal of Robotics and Mechatronics*, 2002. 14(1): p. 78-87.
- [16] Demirel, M., Design of hybrid cable-constrained parallel mechanisms for walking machines. 2018, Izmir Institute of Technology.
- [17] Zi, B., et al., Dynamic modeling and active control of a cable-suspended parallel robot. *Mechatronics*, 2008. 18(1): p. 1-12.
- [18] Tao, Y., X. Xie, and H. Xiong, An RBF-PD Control Method for Robot Grasping of Moving Object, in *Transactions on Intelligent Welding Manufacturing*. 2019, Springer. p. 139-156.
- [19] Homayounzade, M. and A. Khademhosseini, Disturbance Observer-based Trajectory Following Control of Robot Manipulators. *International Journal of Control, Automation and Systems*, 2019. 17(1): p. 203-211.
- [20] Vafaei A., Khosravi M.A., Taghirad H.D., 2011. Modeling and Control of Cable Driven Parallel Manipulators with ElasticCables, Berlin, Pp. 455–464.
- [21] Williams, R.L., P. Gallina, and A. Rossi. Planar cable-direct-driven robots, part i: Kinematics and statics. in *Proceedings of the 2001 ASME Design Technical Conference, 27th Design Automation Conference*. 2001.
- [22] Khosravi, M.A. and H.D. Taghirad, Dynamic modeling and control of parallel robots with elastic cables: singular perturbation approach. *IEEE Transactions on Robotics*, 2014. 30(3): p. 694-704.

- [23] Williams II, R.L. Parallel robot projects at ohio university. In Workshop on fundamental issues and future research directions for parallel mechanisms and manipulators, Quebec City, Canada. 2002.
- [24] Williams, R.L., P. Gallina, and J. Vadia, Planar Translational Cable- Direct- Driven Robots. Journal of Robotic Systems, 2003. 20(3): p. 107-120.
- [25] Errouissi, R., Ouhrouche, M. & Chen, W-H. (2010). Robust Nonlinear Generalized Predictive Control of a Permanent Magnet Synchronous Motor with an Anti-Windup Compensator. In IEEE International Symposium on Industrial Electronics (ISIE).
- [26] Vafaei, A., M.A. Khosravi, and H.D. Taghirad. Modeling and control of cable driven parallel manipulators with elastic cables: Singular perturbation theory, in International Conference on Intelligent Robotics and Applications. 2011. Springer.

Contribution of Individual Authors to the Creation of a Scientific Article (Ghostwriting Policy)

The authors equally contributed in the present research, at all stages from the formulation of the problem to the final findings and solution.

Sources of Funding for Research Presented in a Scientific Article or Scientific Article Itself

No funding was received for conducting this study.

Conflict of Interest

The authors have no conflicts of interest to declare that are relevant to the content of this article.

Creative Commons Attribution License 4.0 (Attribution 4.0 International, CC BY 4.0)

This article is published under the terms of the Creative Commons Attribution License 4.0

https://creativecommons.org/licenses/by/4.0/deed.en_US